Exchange bias and spin-phonon coupling in complex glassy layered perovskite $SrLaMn_{0.5}Ni_{0.5}O_4$

Cite as: AIP Advances **8**, 101423 (2018); https://doi.org/10.1063/1.5043037
Submitted: 05 June 2018 . Accepted: 01 October 2018 . Published Online: 10 October 2018

Ranjana R. Das, P. Neenu Lekshmi, and P. N. Santhosh

Exchange bias and spin-phonon coupling in complex glassy layered perovskite $SrLaMn_{0.5}Ni_{0.5}O_4$

Ranjana R. Das,[a] P. Neenu Lekshmi, and P. N. Santhosh
Department of Physics, Indian Institute of Technology Madras, Chennai 600 036, India

(Received 5 June 2018; accepted 1 October 2018; published online 10 October 2018)

In the present work, single-layered polycrystalline Ruddlesden-Popper oxide, $SrLaMn_{0.5}Ni_{0.5}O_4$ (SLMNO) has been synthesized and characterized. X-ray diffraction and Raman spectroscopy revealed tetragonal crystal structure (*I4/mmm*) with lattice parameters of $a = b = 3.8388$ (4) Å and $c = 12.5593$ (2) Å. XPS analysis confirms Mn^{4+}/Ni^{2+} as the major valance state in SLMNO. Temperature evolution of dc magnetization suggests a ferromagnetic ordering below 130 K followed by a glassy like behaviour below 13 K. The ac susceptibility measurement corroborates the dc magnetization data and confirms cluster glass behavior at lower temperatures. Interestingly, SLMNO exhibits a negative exchange bias of ~ 0.075 kOe at 5 K under field cooling of 50 kOe and also shows the existence of spin-phonon coupling.
https://doi.org/10.1063/1.5043037

INTRODUCTION

La_2NiMnO_6 (LNMO) is a ferromagnetic (FM) insulator in the category of manganate double perovskites with a highest Curie temperature (Tc~280 K).[1–3] Because of being a possible contender for spintronic material as well for its multiferroic behavior, LNMO has been considered as an exciting compound.[2] The evolution of the physical properties with the dimensionality is found to be of interest recently.[4–7] Compared to the 3D double perovskite the quasi-2D layered version of perovskites, Ruddlesden-Popper ((A′O)- $(ABO_3)_n$, n = 1, 2, ... A′= alkali earth, A = rare earth metal and B = transition metals) type compounds, exhibits natural 2D perovskite layers and is not yet explored to that extent.[8] Ruddlesden-Popper (RP) n=1 $SrLaNi_{0.5}Mn_{0.5}O_4$ (SLMNO) was first reported by Millburn *et al.* and proposed antiferromagnetic ordering of Mn^{3+} and high spin (HS) Ni^{3+} ions.[9] Later, Hong *et al.* showed antiferromagnetic interaction between localized ferromagnetically ordered regions due to a partial ordering of Mn^{4+}/Ni^{2+} atoms and with frustrated spins of Mn^{4+}/Ni^{2+} disordered regions.[10] In the present work we have revisited RP n = 1 SLMNO and have carried out in depth analysis on dc and ac magnetization and temperature evolution of Raman spectra. We found first time exchange bias effect and spin-phonon coupling in single layered RP SLMNO compound.

EXPERIMENTAL DETAILS

Polycrystalline compound SLMNO was prepared by sol-gel method using stoichiometric amount of analytical grade La_2O_3, $Sr(NO_3)_2$, $Ni(NO_3)_2{\cdot}6H_2O$ and $Mn(CH_3COO)_2$. The precursor powder is calcined at various temperatures ranging from 1073 – 1373 K with intermediate grindings. Powder X-ray diffraction (XRD) experiment was done using PANalytical X'pert Pro X-ray diffractometer with Cu-K_α radiation (λ=1.5406 Å). Rietveld refinement of the powder XRD data was performed using FULLPROF program. X-ray photoelectron spectroscopy (XPS) analysis was carried out on a PHOIBOS 100MCD analyzer (SPECS) using with Mg-Kα as the X-ray source radiation.

[a]email: ranjanaiitm@gmail.com

Magnetization measurements were carried out using SQUID-VSM magnetometer (Quantum Design, USA) in the temperature (T) range of 5–350 K and in magnetic fields up to 70 kOe. The Raman spectra were recorded in the 180° backscattering geometry using a ~488 nm excitation of air-cooled Argon Ion laser (Labram Micro-Raman Spectrometer).

RESULT AND DISCUSSIONS

Rietveld refinement of XRD pattern at 300 K confirms tetragonal structure with *I4/mmm* space group (No. 124). The obtained lattice parameters are a = b = 3.8388 (4) Å and c =12.5593 (2) Å with reliability factors such as R_p, R_{wp}, and χ^2 are obtained as 2.57 %, 3.60 % and 3.82, respectively, which is in excellent agreement with the reported ones.[9,10]

Temperature variation of Zero Field Cooled (ZFC) and Field Cooled (FC) dc magnetization, M vs T, under 100 Oe is shown in Fig. 1(a). ZFC exhibits a broad peak around 130 K (T_p) which resembles a transition from paramagnetic to an ordered magnetic state, and an additional transition at lower temperature (~13 K) is observed which will be confirmed from ac susceptibility measurement. The inverse of dc magnetic susceptibility ($1/\chi$) vs. T at 100 Oe [Fig. 1(a)] exhibits a Curie-Weiss (CW) behavior above 185 K, $\chi^{-1} = (T - \theta_P)/C$, where C = 2.29 (emu.K/mol) and θ_p = 133 K are CW constant and the CW temperature respectively. The positive value obtained for θ_P suggesting towards the dominant ferromagnetic interactions. In Fig. 1(a) the linear nature of M vs H curve at 300 K confirms paramagnetic nature of the sample whereas 5 K magnetization shows a soft hysteresis with a coercivity of ~ 200 Oe.

The Mn 2p XPS spectra obtained for SLMNO along with the core level Mn $2p_{3/2}$ peak fit are shown in Fig. 1(b) which shows a good agreement with the value reported for Mn^{4+} $2p_{3/2}$ core level.[11] Note that because of partial overlap of the Ni $2p_{3/2}$ and La $3d_{3/2}$ peaks, Ni $2p_{3/2}$ cannot be resolved

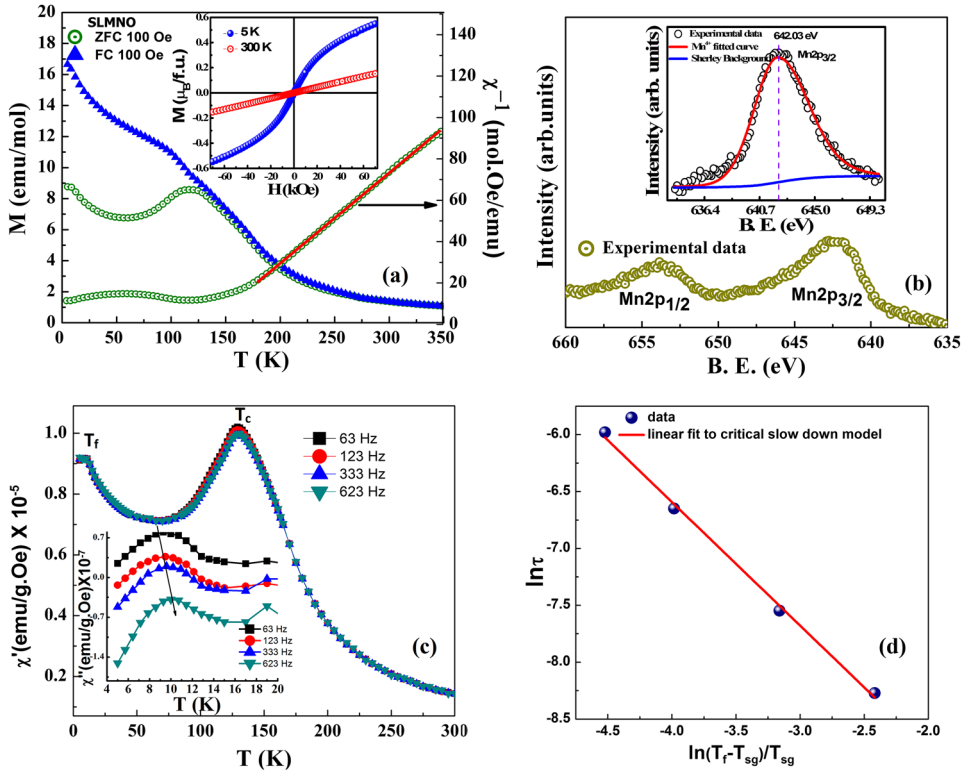

FIG. 1. (a) M (T) under 100 Oe along with 1/χ (T) and Curie-Weiss fit. Inset: M (H) at 5 and 300 K. (b) Mn-2p core level XPS spectra. Inset: Mn-$2p_{3/2}$ core level peak fitting. (c) χ' (T) at different frequencies under an applied ac field of 3 Oe. Inset: $\chi''(T)$ showing the lower temperature peak shift. (d) ln τ vs. ln $((T_f\text{-}T_{sg})/T_{sg})$ with critical slow down model fit.

accurately.[12] Thus from Mn $2p_{3/2}$ analysis, we consider Mn^{4+} and Ni^{2+} combination as predominant oxidation states in SLMNO corroborates the report of Hong *et al.*[10] by XANES spectroscopy studies.

The ac susceptibility measurements were carried out at various frequencies ranging from 63 Hz to 623 Hz at a constant amplitude of the 3 Oe ac field. The temperature variation of both in-phase, $\chi'(T)$ is presented in Fig. 1(c), which exhibit a high temperature maxima at 130 K followed by a low temperature maxima around 10 K at 623 Hz. The frequency independent maxima at 130 K signatures the presence of strong ferromagnetic interaction and hence the transition can be considered as paramagnetic to ferromagnetic transition, (T_C). However, the presence of frequency dependent transition at 10 K (T_f) which is more clearly visible in χ'' (T) (shown in the inset Fig. 1(c)) confirms the low temperature glassy behavior in SLMNO.[13,14] The frequency dependence of T_f can be described using the critical slowing down model as:

$$\tau_f = \tau_0 \left(\frac{T_f - T_{sg}}{T_{sg}} \right)^{-z\vartheta}, \tag{1}$$

where, τ_0 is the microscopic spin-flip time, $T_{sg} = 9.2$ K is the spin glass temperature when $f \rightarrow 0$ and $z\vartheta$ is the critical exponent.[15] Equation (1) is validated in Fig. 1(d) where ln f is plotted as a function of ln $[(T_f - T_{sg})/T_{sg}]$ and the values obtained for τ_0 and $z\vartheta$ are 1.7×10^{-5}s and 1.08 (03), respectively. For a spin-glass system, $\tau_0 = 10^{-13}$ s and $z\vartheta$ typically lie between 4 and 12, the higher value of τ_0 and lower value of $z\vartheta$ are characteristics of randomly oriented magnetic clusters. Thus the obtained value from critical slowing down model supports lower temperature magnetic cluster glass phase in SLMNO.

The exchange bias (EB) field (H_{EB}) is defined by the mean value of the H_{C1} and H_{C2}, i.e.

$$H_{EB} = \left(\frac{H_{C1} + H_{C2}}{2} \right) \text{and } H_C = \left(\frac{H_{c1} - H_{c2}}{2} \right), \tag{2}$$

where H_{C1} and H_{C2} are positive and negative coercive fields respectively and H_C is the coercivity field of the hysteresis loop. Conventional EB measurements comprise the collection of magnetic hysteresis loop at a particular temperature in FC protocol. Here for the FC process, the sample was cooled in an applied magnetic field of 50 kOe from 300 to 5 K; then the hysteresis loop was measured at 5 K between ±70 kOe. In contrast to the usual ZFC hysteresis loop (centered at zero fields, inset Fig. 1(a)), the FC hysteresis loop shifts towards the negative direction of field axis and the positive direction of magnetization axis, suggesting the existence of EB effect. An enlarged view of the central region of the hysteresis loops measured at 5 K with positive and negative cooling fields (FC ± 50 Oe) is shown in Fig. 2(a). Compounds with intrinsic EB will exhibit significant hysteresis loop shift towards negative magnetic field axis with positive cooling field and vice versa with the negative cooling field. SLMNO exhibits hysteresis loop shifts to opposite field direction corresponding to applied cooling fields and H_{EB} value ~ -0.075 kOe is obtained under a cooling field of 50 kOe. Fig. 2(b) shows the

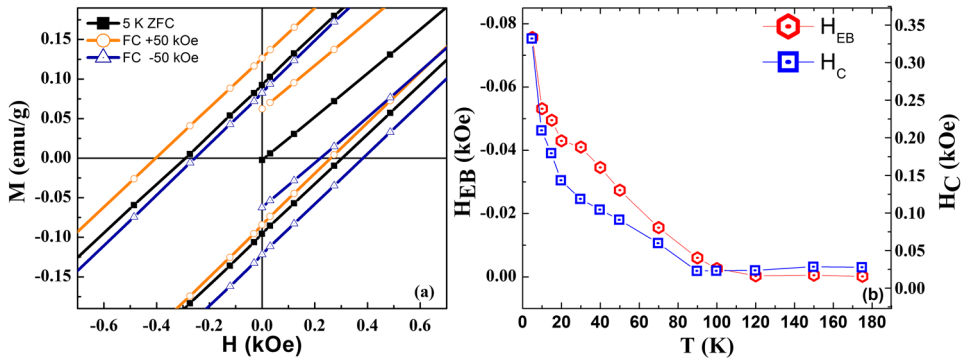

FIG. 2. (a) Zoomed view of ZFC and FC M (H) at 5 K in the range ±70 kOe (b) Temperature variation of the FC H_{EB} and H_C under 50 kOe.

temperature variation of H_{EB} and H_C from 5 – 180 K. Though, the ferromagnetic transition in the present compound, is observed at 134 K, the EB effect is visible only below 100 K.

According to the group theory, structure with tetragonal *I4/mmm* symmetry allows four Raman active modes (2 A_{1g} + 2 E_g). Two A_{1g} modes correspond to stretching vibrations along *z*-axis: (i) (Mn/Ni) – O (2) [A_{1g} (1)], and (ii) (Sr/La) – O (2) [A_{1g} (2)], where O (2) corresponds to apex oxygen atoms. Two doubly degenerated E_g modes represents the vibrations of Sr/La and O (2) along the *xy* plane. Since Mn/Ni and planar oxygen atoms O (1) are at centers of symmetry, their vibrations are not Raman active.

To explore the temperature evolution of vibrational modes, Raman scattering measurements were performed from 300 K down to 100 K, wherein the ferromagnetic transition is also involved. Temperature evolution of Raman spectra [Fig. 3(a)] clarifies that there is no change in spectral signature within the measured temperature range and hence confirms that SLMNO maintains its symmetry down to 100 K. Fig. 3(b) shows Raman spectrum at 110 K along with the deconvoluted peaks assuming the Lorentzian profile of the peaks. Pandey *et al.* reported the A_{1g} modes in layered perovskite around 410 cm^{-1} [A_{1g} (2)] and 630 cm^{-1} [A_{1g} (1)] and E_g modes at 280 and 470 cm^{-1}.[16] Thus the two sharp modes observed in the present compound around 484 and 692 cm^{-1} can be considered as the two A_{1g} modes and other two around 278 and 589 cm^{-1} as E_g modes respectively.

In the absence of structural phase transitions, the other major sources contributing to the temperature dependence of the phonon frequency are: (i) anharmonicity,[17] and (ii) spin-phonon coupling.[18] The variation of peak position as a function of temperature is fitted with an anharmonic model for the temperature dependence of wave number

$$\omega(T) = \omega(0) - c\left(1 + \frac{2}{e^{x-1}}\right), \tag{3}$$

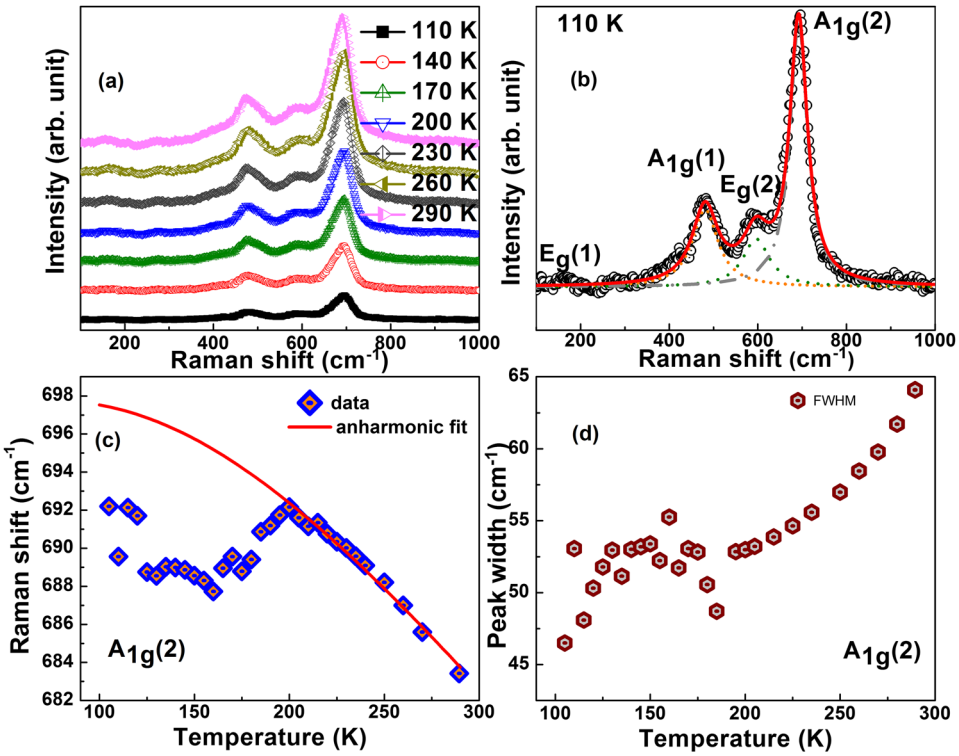

FIG. 3. (a) Raman spectra measured in the temperature range of 290–100 K. (b) Raman spectrum at 110 K displaying peaks at ~692 cm^{-1}, 594 cm^{-1}, and 484 cm^{-1} (dotted red line). (c) Temperature dependence of A_{1g} (1) mode position with anharmonic model fitted using eq. (3). (d) Temperature dependence of A_{1g} (1) mode line width.

where $x = \hbar\omega_0/(2k_BT)$; ω (T) and ω (0) are Raman frequency at temperature T K and 0 K, respectively. ω_0 is the characteristic frequency of the mode, 'c' is adjustable parameters. Temperature evolution of A_{1g} (1) mode position along with the fitted curve using equation (3) is shown in Fig. 3(c). The fitted parameters are ω_0 = 737.27 (1.52) cm^{-1} and c = 39.41 (1.29). Usually, on decreasing temperature, Raman spectra show hardening of peak position and follow the anharmonic model, if there is no structural phase transition. However, SLMNO shows deviation of A_g(1) mode from the anharmonic behavior below 200 K and is attributed to spin-phonon coupling and similar kind of mode softening is also observed in frustruted double perovskite system.[19] Full width at half maxima (FWHM) is another important parameter obtained from the analysis of Raman spectra which is a measure of the phonon lifetime. Raman line widths are expected to decrease with a decrease in temperature. The anomalous behavior of line widths of A_{1g} (1) mode was also observed below 200 K [Fig. 3(d)] confirming spin-phonon coupling in SLMNO.

Thermomagnetic analysis [dc and ac] confirms ferromagnetic transitions at 130 K followed by cluster glass transition at 13 K. This behavior indicates the presence of competing ferromagnetic and antiferromagnetic magnetic interactions at lower temperatures. The XPS analysis confirms the existence of Mn^{4+}/Ni^{2+} spin state combinations. The 180° superexchange interactions between Mn^{4+} - O - Ni^{2+}, favors ferromagnetic coupling.[3,20] However, the experimentally observed maximum magnetization at 5 K under 70 kOe is ~ 0.55 μ_B/f.u. which is much lower than the spin-only value of magnetization ~2.5 μ_B/f.u with five unpaired spins [Mn^{4+}/Ni^{2+}]. This massive reduction in magnetization might be because of the quasi 2D RP layered structure where the perovskite layers (ABO_3) are stacked between rock salt layers (AO) along the crystallographic c-axis. The size of the cations at B-site influence the cell parameter *a*, whereas A site cations prominently affect the lattice parameter *c*. The lattice parameters obtained from the structural refinement are $a = b = 3.8388$ Å and $c = 12.5593$ Å. Thus the separation between the perovskite layers are larger which in turn reduces the interaction between adjacent perovskite layers. Hence, the interlayer magnetic interaction will be very weak. Moreover, the quasi 2D layered structure does not provide a long range ordering of Mn^{4+}/Ni^{2+} ions in the ab plane as in 3D network.[21] As a result, there are the possibilities for Mn^{4+}-O-Mn^{4+}/Ni^{2+}-O-Ni^{2+} antiferromagnetic (AFM) interactions arising either from the antiferromagnetic boundaries of locally ordered clusters or from the disordered regions.[10] Additionally, the layer by layer magnetic contributions will be different which may also affect the overall magnetization value. The origin of EB phenomenon can be attributed to the existence of competitive FM and AFM interactions within individual layers. Further, we have obtained a higher value of effective paramagnetic moment in the present compound (μ_{eff} = 4.27 μ_B/f.u) than the Mn^{4+} and Ni^{2+} combinations (3.87 μ_B).[20] Thus the higher paramagnetic moment might be due to the co-existence of paramagnetic moments with short range ferromagnetic clusters of Mn^{4+}-O-Ni^{2+} in the temperature regime considered for CW fit. The spin-phonon coupling is also observed much above the magnetic transition (130 K) confirming the presence of FM clusters in the paramagnetic region.

CONCLUSIONS

Detailed magnetic and Raman spectral studies were carried out on quasi 2D RP (n=1) tetragonal $SrLaMn_{0.5}Ni_{0.5}O_4$ compound. EB about -0.075 kOe is observed at 5 K under a cooling field of 50 kOe, and ac susceptibility analysis confirms a cluster glass transition at lower temperatures below 13 K. The ferromagnetic perovskite layer contains antiferromagnetic patches due to antiphase boundaries and disordered regions which will provide competing interactions in the perovskite layers, in turn responsible for the observed EB in the RP phase. The interaction between clusters is not strong since the cationic ordering, as well as the magnetization, differ from layer to layer where the interlayer interactions are very weak. Further, we have observed spin-phonon coupling below 200 K.

ACKNOWLEDGMENTS

P.N.S acknowledges Council of Scientific and Industrial Research (CSIR), India for financial support (Project No. 03(1214)/12/EMR-II). Authors would like to thank IIT Madras for the SQUID VSM measurements. PNL thanks to DST National Post Doctorial fellowship [PDF/2017/001826].

[1] M. N. Iliev, M. M. Gospodinov, M. P. Singh, J. Meen, K. D. Truong, P. Fournier, and S. Jandl, Journal of Applied Physics **106**(2), 023515 (2009).
[2] Y. Guo, L. Shi, S. Zhou, J. Zhao, and W. Liu, Applied Physics Letters **102**(22), 222401 (2013).
[3] R. I. Dass, J. Q. Yan, and J. B. Goodenough, Physical Review B **68**(6), 064415 (2003).
[4] A. Cammarata and J. M. Rondinelli, Physical Review B **92**(1), 014102 (2015).
[5] R. G. Palgrave, P. Borisov, M. S. Dyer, S. R. McMitchell, G. R. Darling, J. B. Claridge, M. Batuk, H. Tan, H. Tian, J. Verbeeck, J. Hadermann, and M. J. Rosseinsky, J Am Chem Soc **134**(18), 7700–7714 (2012).
[6] J. Xue, Q. Liao, W. Chen, H. J. M. Bouwmeester, H. Wang, and A. Feldhoff, J. Mater. Chem. A **3**(37), 19107–19114 (2015).
[7] M. E. Ghazi, P. D. Spencer, S. B. Wilkins, P. D. Hatton, D. Mannix, D. Prabhakaran, A. T. Boothroyd, and S. W. Cheong, Physical Review B **70**(14), 144507 (2004).
[8] S. N. Ruddlesden and P. Popper, Acta Crystallographica **10**(8), 538–539 (1957).
[9] J. E. Millburn and M. J. Rosseinsky, Journal of Materials Chemistry **8**(6), 1413–1421 (1998).
[10] K. Hong, Y.-U. Kwon, D.-K. Han, J.-S. Lee, and S.-H. Kim, Chemistry of Materials **11**(7), 1921–1930 (1999).
[11] W. Yang, J. Zhang, Q. Ma, Y. Zhao, Y. Liu, and H. He, Sci Rep **7**(1), 4550 (2017).
[12] K. Wissel, J. Heldt, P. B. Groszewicz, S. Dasgupta, H. Breitzke, M. Donzelli, A. I. Waidha, A. D. Fortes, J. Rohrer, P. R. Slater, G. Buntkowsky, and O. Clemens, Inorganic Chemistry **57**(11), 6549–6560 (2018).
[13] H. S. Nair, T. Chatterji, and A. M. Strydom, Applied Physics Letters **106**(2), 022407 (2015).
[14] B. Roy, A. Poddar, and S. Das, Journal of Applied Physics **100**(10), 104318 (2006).
[15] J. A. Mydosh, Rep Prog Phys **78**(5), 052501 (2015).
[16] P. K. Pandey, R. J. Choudhary, D. K. Mishra, V. G. Sathe, and D. M. Phase, Applied Physics Letters **102**(14), 142401 (2013).
[17] M. Balkanski, R. F. Wallis, and E. Haro, Physical Review B **28**(4), 1928–1934 (1983).
[18] E. Granado, A. García, J. A. Sanjurjo, C. Rettori, I. Torriani, F. Prado, R. D. Sánchez, A. Caneiro, and S. B. Oseroff, Physical Review B **60**(17), 11879–11882 (1999).
[19] A. F. García-Flores, H. Terashita, E. M. Bittar, R. F. Jardim, and E. Granado, Journal of Raman Spectroscopy **45**(2), 193–196 (2013).
[20] A. Wold, R. J. Arnott, and J. B. Goodenough, Journal of Applied Physics **29**(3), 387–389 (1958).
[21] T. Chakraborty, C. Meneghini, A. Nag, and S. Ray, Journal of Materials Chemistry C **3**(31), 8127–8131 (2015).